

Probing magnetic order in ultracold lattice gases

G. De Chiara,¹ O. Romero-Isart,² and A. Sanpera^{1,3}

¹*Física Teòrica: Informació i Processos Quàntics,
Universitat Autònoma de Barcelona, E-08193 Bellaterra, Spain*

²*Max-Planck-Institut für Quantenoptik,
Hans-Kopfermann-Strasse 1, D-85748, Garching, Germany.*

³*ICREA, Institució Catalana de Recerca i Estudis Avançats, E08011 Barcelona*

Abstract

The simulation of quantum magnetism with ultracold lattice gases is one of the next challenges in the field of ultracold atoms. We propose a method to measure directly the *order parameter* of non trivial antiferromagnetic quantum phases in a non demolishing way. This atom-light interface gives access to spatially resolved spin correlations. Such probing scheme allows one to univocally characterize strongly correlated magnetic systems simulated with ultracold atoms in optical lattices. As a proof of principle, we apply our method to detect the complete phase diagram of the rotational invariant spin-1 chain.

PACS numbers: 37.10.Jk, 75.10.Pq, 42.50.-p

The possibility of using ultracold gases as quantum simulators, i.e. an experimental system that mimics simple models of condensed matter, high energy physics or quantum chemistry, was boosted by the seminal realization of Bose-Einstein condensate in alkaline atoms[1]. Since then, the field has progressed enormously, both theoretically and experimentally, moving from the weakly-correlated regime towards the strongly-correlated regime [2, 3]. This has been accomplished mainly by the use of optical lattices and Feshbach resonances. A forthcoming step is the simulation of quantum magnetism in ultracold lattice gases. Recent experiments, beating some of the challenging experimental requirements to achieve this goal, have already been reported [4].

One of the major difficulties confronted by such quantum simulators is not only the preparation but also the faithful detection of the many-body state. A full tomographic reconstruction of it is, generally, unrealistic since it demands a number of measurements that scales exponentially with the number of particles. In quantum many-body systems, instead, one is generally interested in the effects produced by interactions and quantum correlations between their constituents. These are usually reflected by a set of *order parameters* given by local operators with a non vanishing expectation value. Such a set reveals the ordering (symmetries) of the ground state. Landau introduced the order parameter concept as a way to quantify the dramatic transformation of matter at a (classical) phase transition. Within the Landau theory, a phase is associated to a given broken symmetry and a phase transition is pointed out by a drastic change of the order parameter value. In passing, notice that there exist also quantum phases like e.g. topological, whose symmetries are non local but global and, therefore, cannot be described by local order parameters.

In some cases, it is possible to measure directly the order parameter of the simulated system, for example the gap in the Bose-Hubbard model or the magnetization in a ferromagnetic state, but often this is not the case. Detection of antiferromagnetic ground states requires the knowledge of spin-spin correlations which frequently demands spatial resolution of the detection probe. Standard detection methods of spin-spin correlations obtained via noise-correlations [5, 6] or Bragg scattering [7], give only a limited information on the magnetic ordering and have two major drawbacks: first, the sample is destroyed during the imaging process and second, spatial resolution cannot be achieved without single atoms detectors.

A new technique for the detection of magnetic correlations in optical lattices, based on

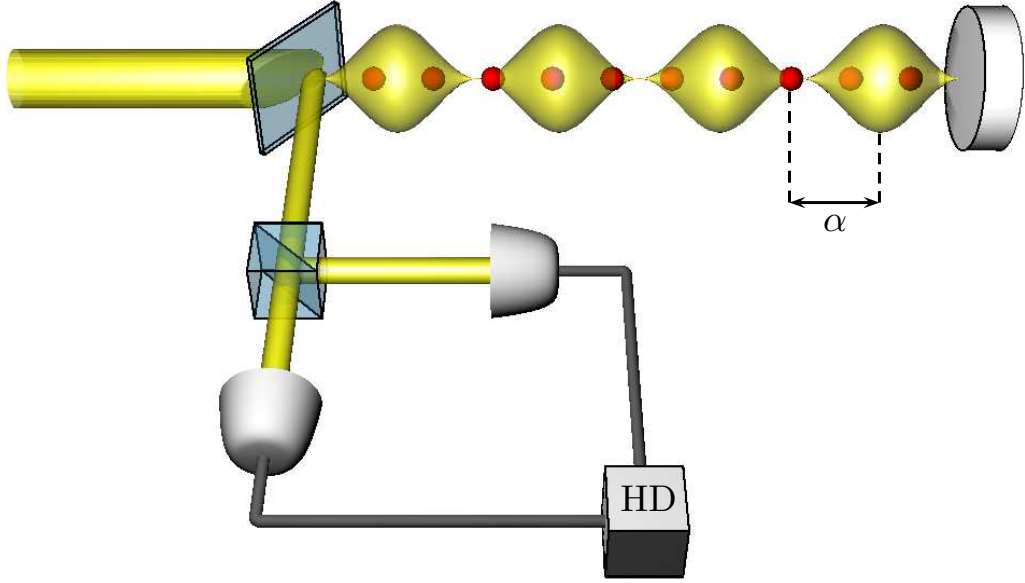


FIG. 1: Schematic detection setup: atoms placed in an optical lattice of periodicity $d/2$ (not shown) are illuminated by a laser beam in a standing wave configuration (yellow region) shifted by α from the optical lattice configuration. The output light is redirected through a polarimeter which measures its polarization through a homodyne detection (HD).

quantum polarization spectroscopy (QPS), can overcome these limitations. The method, reported in Ref. [8] and depicted schematically in Fig. 1, takes advantage of the Faraday effect occurring when off-resonant light interacts with an atomic system with internal spin degrees of freedom. In general, when a polarized light pulse is sent to a sample of such atoms in an optical lattice, the light polarization couples to the atomic spin, and as a result of the interaction, the polarization rotates proportionally to the sample magnetization. By measuring the polarization of the outgoing light one can, therefore, reconstruct the magnetization of the many-body system as well as its fluctuations. For an antiferromagnetic state, possessing non trivial spin-spin correlations, the polarization rotation of light is trivially zero and a probe with spatial resolution is needed. This can be achieved by using a standing wave configuration for the probing light as shown in Fig. 1. The periodicity of the probing standing wave and its displacement with respect to the optical lattice potential (indicated by α in Fig. 1) are parameters that can be straightforwardly controlled [8]. Such controls

provide access to the system response and address certain type of spin-spin correlations which are present in antiferromagnetic phases.

An open question is whether this method can be used to characterize magnetic quantum phases, that is, whether one can measure order parameters of strongly correlated systems. Here we propose a measure, with the use of QPS, that can be used to detect some local order parameters in strongly-correlated quantum magnetic systems. We illustrate our method with the bilinear-biquadratic spin-1 chain and show that the analysis of the QPS signal corresponding to light probes with different periodicity and different shift α , lead to the relevant magnetic order parameters. We emphasize that those order parameters cannot be obtained by measuring the magnetic structure factor alone. Recently an alternative non demolishing technique for imaging spin states in optical lattices has been put forward [9].

To be more precise, in the QPS scheme the polarization of the incoming light is rotated as a consequence of the interaction with the effective angular momentum generated by the atomic magnetic moments: $J_z^{eff} = 1/\sqrt{L} \sum_n c_n S_{zn}$. Here, S_{zn} is the z component of the spin at site n , and L is the total number of spins. In the limit of strongly localized atomic Wannier functions, the coefficients c_n , related to the standing wave intensity profile, can be approximated by: $c_n = 2 \cos^2[k_P d(n - \alpha)]$ where we defined the dimensionless shift α between the standing wave and the atomic lattice, and k_P is the wave number of the probing laser, and d the lattice spacing. As reported in Appendix A, the angular momentum J_z^{eff} is mapped onto the quantum fluctuation X of the light polarization in a direction orthogonal to the incoming one. The result of the mapping is (see also [20]):

$$X_{out} = X_{in} - \kappa J_z^{eff} \quad (1)$$

where X_{in} (X_{out}) is the quadrature of the incoming (outgoing) light and the coupling constant κ depends on the optical depth of the atomic sample and on the probability of exciting an atom due to the probe. By measuring X_{out} , using homodyne detection, and by the knowledge of the statistical properties of the incoming light, one is able to directly measure the complete distribution of the effective angular momentum J_z^{eff} .

Thus, in the QPS one has access to the mean effective angular momentum $\langle J_z^{eff} \rangle$ and the variance $\varepsilon(k_P, \alpha) \equiv (\Delta J_z^{eff})^2$ (as well as higher moments). The quantity $\langle J_z^{eff} \rangle$ for $k_P = 0$, is proportional to the spontaneous magnetization and hence is the order parameter for a ferromagnetic phase. In order to discriminate different antiferromagnetic phases, for which

$\langle J_z^{eff} \rangle = 0$, we employ the variance which gives us access to magnetic correlations:

$$\varepsilon(k_P, \alpha) = \frac{1}{L} \sum_{nm} c_m c_n \mathcal{G}_z(m, n). \quad (2)$$

where $\mathcal{G}_z(m, n) \equiv \langle S_{zm} S_{zn} \rangle - \langle S_{zm} \rangle \langle S_{zn} \rangle$ is the two-point correlation function. As noticed in [10], in the case of an antiferromagnetic sample for which the net magnetization is zero, the magnetic structure factor, defined as $S(q) = 1/L \sum_{mn} \exp[iqd(m-n)] \langle S_{zm} S_{zn} \rangle$, can be connected to the average over α of the output signal:

$$\bar{\varepsilon}(k_P) \equiv \int d\alpha \varepsilon(k_P, \alpha) = \frac{1}{2} S(2k_P) \quad (3)$$

In principle, by averaging over the phase shift α one loses some information on the correlations. In this work instead we assume an accurate control on the shift α and we introduce the key quantity:

$$\Delta\varepsilon(k_P, \alpha_1, \alpha_2) \equiv \varepsilon(k_P, \alpha_1) - \varepsilon(k_P, \alpha_2) \quad (4)$$

which is the difference of the signal with fixed wavevector k_P at two different phase shifts. By appropriately choosing the parameters k_P, α_1, α_2 , this quantity can be linked to the local order parameters of different antiferromagnetic phases. We now illustrate the power of our method in the specific case of a one dimensional spin-1 chain realized with ultracold atoms in optical lattices.

Spin-1 atoms confined in a deep optical lattice are well described by the Bose-Hubbard Hamiltonian [11]. For unit filling and for sufficiently small tunneling the system is in a Mott insulator state with one atom per site. Virtual tunneling of the atoms between neighboring sites gives rise to an effective magnetic interaction described by the bilinear-biquadratic Hamiltonian [11]:

$$H_{BB} = \sum_i \cos(\theta) \mathbf{S}_i \cdot \mathbf{S}_{i+1} + \sin(\theta) (\mathbf{S}_i \cdot \mathbf{S}_{i+1})^2 \quad (5)$$

Hamiltonian (5) is derived within second order perturbation theory in the tunneling rate and the angle $\theta \in [-\pi; \pi]$ depends only on the two-body short range atom-atom interaction. This model is characterized by a rich phase diagram depending on the angle θ and has been extensively studied in the literature, see [12–18] and references therein. Let us review the phase diagram:

The ferromagnetic phase.- For $\pi/2 < \theta < 5\pi/4$, the ground state is ferromagnetic exhibiting a spontaneous magnetization, which serves as a local order parameter.

For the remaining values of θ , the ground state is antiferromagnetic with no net magnetization but different quantum phases:

The critical phase.- In the interval $\pi/4 < \theta < \pi/2$ the system is gapless due to soft collective modes at momenta $q = 0, \pm 2\pi/(3d)$. The ground state spin-spin correlation functions $\langle S_{zi} S_{z(i+r)} \rangle$ show period-3 oscillations [18]. In momentum space, this feature emerges as a peak at $q = 2\pi/(3d)$ in the magnetic structure factor $S(q)$. Recently Läuchli et al. [15] have shown that nematic (i.e. quadrupolar) correlations at momentum $q = 2\pi/(3d)$ are enhanced in the critical phase while spin correlations become smaller when increasing θ from 0.2π to 0.5π . Together with the absence of the gap, the enhanced nematic correlations are a distinctive feature of the critical phase.

The Haldane phase.- The interval $-\pi/4 < \theta < \pi/4$ contains for $\theta = 0$ the spin-1 Heisenberg chain and for $\tan(\theta) = 1/3$ the exactly solvable AKLT point [16]. The presence of a gap excludes local quasi long range order and spin correlations decay exponentially. The Haldane phase can be characterized by a hidden topological order parameter, called the string order parameter [19], that cannot be revealed with local measurements.

The dimer phase.- In the region $-3\pi/4 < \theta < -\pi/4$ the ground state is gapped and breaks translational invariance, organizing in slightly correlated dimers. For $-3\pi/4 < \theta < -\pi/2$ it is still under debate whether the system is always dimerized or it becomes nematic. Numerical results [12–15] show that the dimer order parameter, $D = |\langle H_i - H_{i+1} \rangle|$ where $H_i = \cos(\theta) \mathbf{S}_i \cdot \mathbf{S}_{i+1} + \sin(\theta) (\mathbf{S}_i \cdot \mathbf{S}_{i+1})^2$, is different from zero up to values very close to $\theta = -3\pi/4$ giving strong evidence for the absence of the nematic phase.

We employed the density matrix renormalization group (DMRG) [21] to compute the quantities $\varepsilon(k_P, \alpha)$, which depend on all possible two-spin correlations. In Fig. 2 we show $\varepsilon(k_P, \alpha)$ in three different points corresponding to the different antiferromagnetic phases. A common feature of the three phases is the presence of a high peak at $k_P d = \pi/2$ due to the antiferromagnetic order. Apart from this, the plots in the three phases are qualitatively different. In fact, in the critical phase, the signal is characterized by peaks at $k_P d \sim \pi/3$ and $k_P d \sim 2\pi/3$. These resemble the peaks of the magnetic structure factor $S(2k_P)$ [17] and are due to the period-3 oscillations of the correlation functions. These correlations are fundamental for the detection of the critical phase. For $\theta < -\pi/4$ we find the appearance of other small peaks at $k_P d = \pi/4$ and $k_P d = 3\pi/4$ signaling, as we show below, the dimer order. Finally, in the Haldane phase, the signal $\varepsilon(k_P, \alpha)$ lacks of non trivial features for

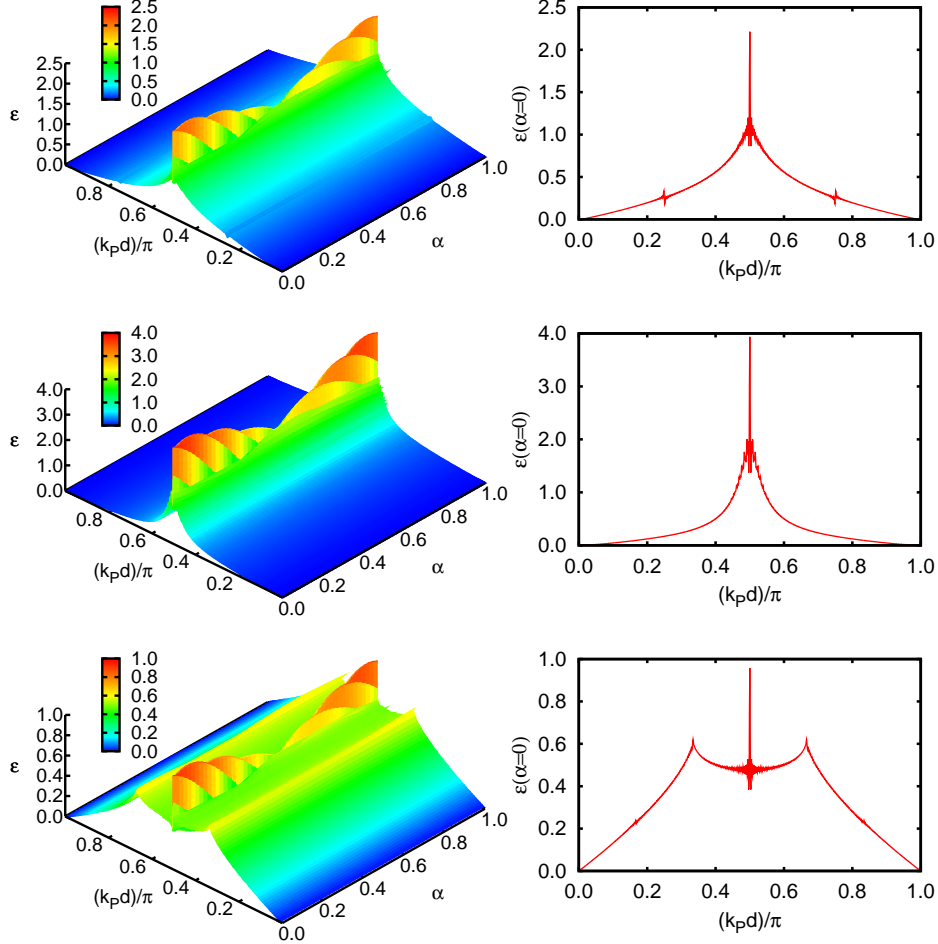


FIG. 2: Left column, the function $\varepsilon(k_P, \alpha)$ for different values of θ in the three phases for $L = 132$: top $\theta = -0.5\pi$ (dimer), middle $\theta = 0$ (Haldane), bottom $\theta = 0.3\pi$ (critical). Right column, the same plots but restricted to $\alpha = 0$.

$k_P d \neq \pi/2$.

We now use the quantity $\Delta\varepsilon(k_P, \alpha_1, \alpha_2)$ introduced in Eq. (4) for the detection of the critical and dimer phase. To see how to choose the parameters k_P, α_1, α_2 , let us consider the critical phase. In this case it is natural to take $k_P = \pi/3d$. Then we study the behavior of $\varepsilon(\pi/3d, \alpha)$ in the critical phase as a function of α . A numerical analysis, reported in Appendix B, shows that the quantity $\varepsilon(\pi/3d, \alpha)$ is a sinusoidal oscillating function of α . The role of correlations at $k_P = \pi/3d$ is optimized by taking the difference between its maximum value at $\alpha_1 = 5/4$ and its minimum at $\alpha_2 = 1/2$. We then introduce $\mathcal{C}_\varepsilon = \Delta\varepsilon(\pi/3d, 5/4, 1/2)$ which we consider as an order parameter for the critical phase. Using the fact that the ground

state is a zero angular momentum eigenstate we obtain:

$$\mathcal{C}_\varepsilon = \frac{1}{L} \sum_{mn} \cos \left[\frac{2\pi}{3}(m+n) + \frac{\pi}{3} \right] \mathcal{G}_z(m, n) \quad (6)$$

The quantity \mathcal{C}_ε is sensitive to correlations which oscillate with a period 3 and represents a footprint of the critical phase. In Fig. 3a we show the signal \mathcal{C}_ε for different values of θ in the antiferromagnetic phase. The results clearly show that the critical phase is very well detected by a positive value of \mathcal{C}_ε . For $\theta = 0.2\pi$, in the Haldane phase and close to the phase transition, we still observe a large positive value, probably due to residual period-3 correlations persisting in the Haldane phase. However, in this point, we find a non negligible dependence with the size of the sample. As shown in the inset of Fig. 3a a finite size scaling suggests that in the thermodynamical limit for $L \rightarrow \infty$ the quantity \mathcal{C}_ε goes to zero as $1/L$ for $\theta = 0.2\pi$, while for the other values of $\theta \geq 0.24\pi$ it converges to a finite value. In Fig. 3a we compare \mathcal{C}_ε with the magnetic structure factor $S(2\pi/3d)$. We confirm the results found in [15] for chains up to $L = 18$: since the maximum is at $\theta \simeq 0.2\pi$, the magnetic structure factor alone is not sufficient to distinguish the critical point at $\theta = 0.25\pi$. As shown in [15], one would also need the quadrupolar structure factor to find the critical point. Our findings indicate that measuring only \mathcal{C}_ε , which behaves as an order parameter, is sufficient to infer the occurrence of the phase transition.

In the dimerized phase, the presence of peaks at $k_P d = \pi/4$ signals the pairing of neighboring spins. By averaging the signal $\varepsilon(k_P, \alpha)$ over α , these peaks disappear. Therefore, these features are not visible in the magnetic structure factor. Following a similar reasoning that leads to the definition of \mathcal{C}_ε , we find that the quantity

$$\mathcal{D}_\varepsilon \equiv \Delta\varepsilon\left(\frac{\pi}{4d}, \frac{1}{2}, \frac{3}{2}\right) = -\frac{1}{L} \sum_{mn} \sin \left[\frac{\pi}{2}(m+n) \right] \mathcal{G}_z(m, n)$$

is suitable for the detection of the dimer phase. The factor $\sin[\pi/2(m+n)]$ ensures that only the pairs of spins with positions m and n of opposite parity contribute to \mathcal{D}_ε . The differential signal \mathcal{D}_ε is therefore an extension to long range correlations of the dimer order parameter D . In Fig. 3b we compare the signal \mathcal{D}_ε and the dimer order parameter D for different values of θ . Similar to D , the quantity \mathcal{D}_ε is significantly different from zero only in the dimerized phase, with the advantage of being experimentally measurable.

The simulation of antiferromagnets with optical lattices can be foreseen in the next generation of experiments with ultracold atoms. Once this is accomplished, the measurement

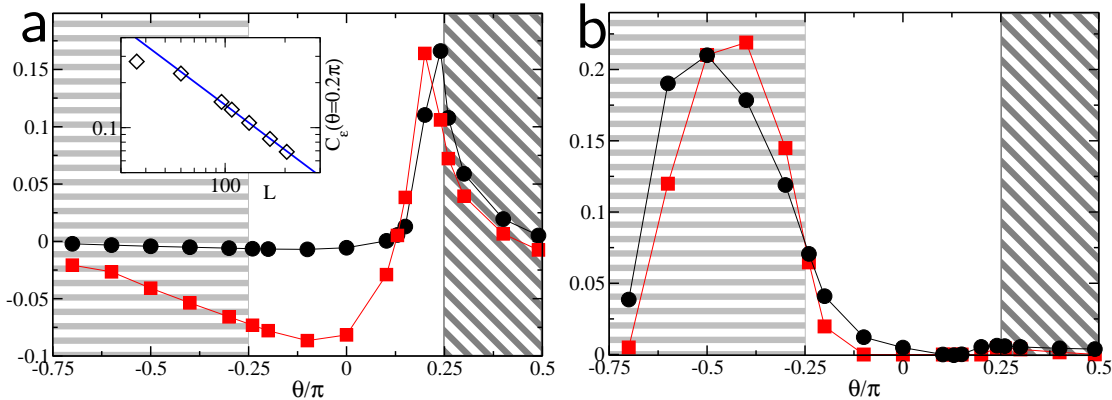


FIG. 3: **a**: The quantity $\mathcal{C}_\varepsilon = \Delta\varepsilon(\pi/3d, 5/4, 1/2)$ (circles) as a function of θ for $L = 132$ and the rescaled magnetic structure factor $[S(2\pi/3d) - 1]/5$ (squares). Inset: finite size scaling of \mathcal{C}_ε for $\theta = 0.2\pi$. The solid line scales as $1/L$. **b**: the quantity $\mathcal{D}_\varepsilon = \Delta\varepsilon(\pi/4d, 1/2, 3/2)$ (circles) for different values of θ for $L = 132$ and the rescaled dimer order parameter $D_R = D/5.38$. In the two plots, we distinguish the model phases with different shading: horizontal lines (dimer), no shading (Haldane), oblique lines (critical).

of order parameters characterizing these phases will be of utmost importance. In this work we proposed the use of QPS for the direct observation of magnetic order parameters in ultracold atoms in optical lattices. As a proof of principle, we have shown that this method allows us to unambiguously reconstruct the rotational invariant spin-1 chain phase diagram. We emphasize that the method is very general and could be applied to other spin models. Notice also that the QPS technique we propose is not based on any previous knowledge of the quantum phase to be characterized, but rather takes advantage of the features displayed by the probing scheme properly optimized. Although we are not able to measure directly the string order parameter in the Haldane phase with second order correlation functions, topological order can in principle be extracted from the higher moments of the output light quadrature. This measure, provided that the shot noise of the incoming light is small, employing for instance squeezed light, adds no experimental effort and will be the subject of future investigations.

Acknowledgments.— We thank P. Massignan, S. Paganelli, M. Rizzi, and U. Schollwöck for discussions. We acknowledge support from the Spanish MICINN (Juan de la Cierva, FIS2008-01236 and QOIT-Consolider Ingenio 2010), Generalitat de Catalunya Grant No.

2005SGR-00343 and the Alexander von Humboldt foundation. We used the DMRG code available at <http://www.dmrp.it>.

Appendix A: The detection scheme

Here we describe in detail the detection scheme based on polarization spectroscopy. We refer the reader to the original works [8, 10] where this method has first been proposed.

As described in the main text and sketched in Fig. 1 of the main text, the scheme consists in shining the atoms with a non resonant probe beam in a standing wave configuration. For light propagating along the z -axis, parallel to the atomic array, light-atom interaction is best expressed using the Stokes parameters defined as:

$$s_1 = \frac{1}{2}(a_x^\dagger a_x - a_y^\dagger a_y) \quad (\text{A1})$$

$$s_2 = \frac{1}{2}(a_y^\dagger a_x + a_x^\dagger a_y) \quad (\text{A2})$$

$$s_3 = \frac{1}{2i}(a_y^\dagger a_x - a_x^\dagger a_y) \quad (\text{A3})$$

where a_x and a_y are the photon annihilation operators with polarization along x and y such that $n_x = a_x^\dagger a_x$ and $n_y = a_y^\dagger a_y$ are the number of photons per unit of time with polarization x and y respectively. Using this definition, the atom-light interaction is described by the Hamiltonian (see for example [20]):

$$H_{AL} = -\kappa s_3 J_z^{eff} \quad (\text{A4})$$

where the coupling constant κ depends on the optical depth of the atomic sample and on the probability of exciting an atom due to the probe. The effective angular momentum J_z^{eff} depends on the intensity profile of the probe beam. In the case of a simple standing wave the effective angular momentum is given by $J_z^{eff} = 1/\sqrt{L} \sum_n c_n S_{zn}$ and the coefficients are defined as

$$c_n = 2 \int dz \cos^2[k_P(z - a)] |w(z - nd)|^2 \quad (\text{A5})$$

where k_P is the wavevector of the probe light, a is a shift and $w(z - nd)$ is the first band Wannier function of the atom centered at lattice position $z = nd$. In the calculations for simplicity we approximate the Wannier functions with delta functions centered at the lattice positions so that the coefficients are now given by $c_n = 2 \cos^2[k_P d(n - \alpha)]$ where we defined the dimensionless shift $\alpha = a/d$.

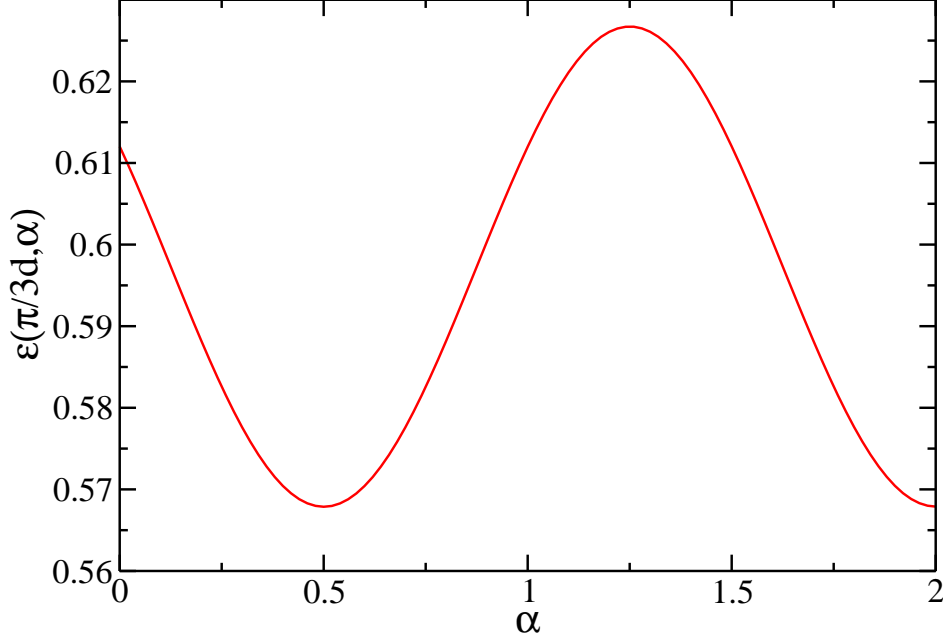


FIG. 4: The quantity $\varepsilon(\pi/3d, \alpha)$ for $\theta = 0.3\pi$ for $L = 132$ as a function of α .

We now assume the incoming light to be strongly polarized along the x direction, i.e. $\langle S_1 \rangle = N_{ph} \gg 1$ where $S_i = \int dt s_i$ and N_{ph} is the beam total number of photons. Using Holstein-Primakoff transformation, we can approximate the other two Stokes operators as two effective conjugated variables: $X = S_2/\sqrt{N_{ph}}$ and $P = S_3/\sqrt{N_{ph}}$ such that

$$[X, P] = \frac{iS_1}{N_{ph}} \sim i. \quad (\text{A6})$$

Integrating out the Heisenberg equation of motion for these light quadratures we get

$$X_{out} = X_{in} - \kappa J_z^{eff} \quad (\text{A7})$$

where X_{in} is the quadrature of the incoming light and X_{out} is the output light emerging from the sample that can be measured using homodyne detection as shown in Fig. 1 in the main text.

Appendix B: The choice of the parameter α

Here we briefly describe how to choose the phase shifts α_1, α_2 for the critical phase order parameter. We study the behavior of $\varepsilon(\pi/3d, \alpha)$ in the critical phase as a function

of α as shown in Fig. 4. The quantity $\varepsilon(\pi/3d, \alpha)$ is a sinusoidal oscillating function of α whose difference $\Delta\varepsilon(\pi/3d, 5/4, 1/2)$ between the maximum at $\alpha_1 = 5/4$ and the minimum at $\alpha_2 = 1/2$ gives twice its amplitude. We take this quantity $\mathcal{C}_\varepsilon = \Delta\varepsilon(\pi/3d, 5/4, 1/2)$ as the corresponding order parameter. In the dimer phase a similar analysis leads to $k_P = \pi/4d, \alpha_1 = 1/2, \alpha_2 = 3/2$.

-
- [1] M. H. Anderson et al., *Science* **269**, 198 (1995); K. B. Davis et al., *Phys. Rev. Lett.* **75**, 3969 (1995).
 - [2] M. Lewenstein et al., *Adv. in Phys.* **56**, 243 (2007).
 - [3] I. Bloch, J. Dalibard, and W. Zwerger, *Rev. Mod. Phys.* **80**, 885 (2008).
 - [4] S. Trotzky et al., *Science* **319**, 295 (2008). P. Medley et al., arXiv:1006.4674
 - [5] E. Altman, E. Demler, and M. D. Lukin, *Phys. Rev. A* **70**, 013603 (2004).
 - [6] S. Fölling, et al., *Nature* **434**, 481 (2005).
 - [7] T. A. Corcovilos, et al., *Phys. Rev. A* **81**, 013415 (2010).
 - [8] K. Eckert, et al., *Nat. Phys.* **4**, 50 (2008).
 - [9] J. Douglas and K. Burnett, arXiv:1007.1899.
 - [10] T. Roscilde, et al., *New. J. Phys.* **11**, 055041 (2009).
 - [11] A. Imambekov, M. Lukin, and E. Demler, *Phys. Rev. A* **68**, 063602 (2003).
 - [12] G. Fáth and J. Sólyom, *Phys. Rev. B* **51**, 3620 (1995).
 - [13] M. Rizzi, et al. *Phys. Rev. Lett.* **95**, 240404 (2005).
 - [14] K. Buchta et al., *Phys. Rev. B* **72**, 054433 (2005).
 - [15] A. Läuchli, G. Schmid, and S. Trebst, *Phys. Rev. B* **74**, 144426 (2006).
 - [16] I. Affleck, et al., *Phys. Rev. Lett.* **59**, 799 (1987).
 - [17] U. Schollwöck, Th. Jolicoeur, and T. Garel, *Phys. Rev. B* **53**, 3304 (1996).
 - [18] G. Fáth and J. Sólyom, *Phys. Rev. B* **44**, 11836 (1991).
 - [19] M. den Nijs and K. Rommelse, *Phys. Rev. B* **40**, 4709 (1989).
 - [20] B. Julsgaard, PhD-thesis, University of Aarhus (2003).
 - [21] S. R. White, *Phys. Rev. Lett.* **69**, 2863 (1992); U. Schollwöck, *Rev. Mod. Phys.* **77**, 259 (2005); G. De Chiara, et al. *J. Comp. Theor. Nanos.* **5**, 1277 (2008).